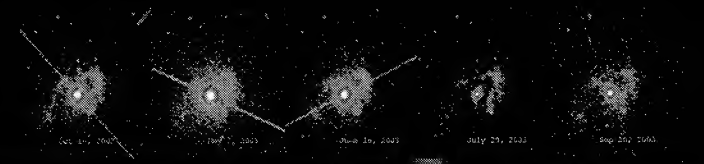


Eta Carinae: X-ray Line Variations during the 2003 X-ray Minimum, and the Orbit Orientation

M. F. Corcoran¹, D. Henley², K. Hamaguchi¹, K. Ishibashi³, J. M. Pittard⁴, J. R. Stevens⁵, & T. R. Gull⁶

¹CRESST /USRA/GSFC, ²The University of Georgia, ³NWRA/CoRA, ⁴The University of Leeds, ⁵The University of Birmingham, ⁶ASD/NASA/GSFC

E-mail: corcoran@milkyway.gsfc.nasa.gov



The observations: 51HLGS 100 keV pointings (A14) near the X-ray minimum/periastrom passage of Eta Car in mid-2003, plus an earlier (A03) pointing near apastron

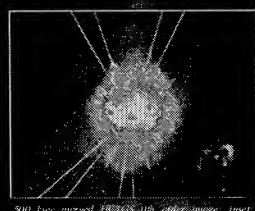
© 2004 The American Astronomical Society

Why this is Important:

- ⇒ The future evolution of Eta Car will be dramatic: a supernova (or hypernova + black hole)
- ⇒ The evolution is highly contingent on mass and angular momentum changes and instabilities
- ⇒ The presence of a companion can serve to trigger instabilities and provide pathways for mass and angular momentum exchange loss

X-rays as a Key Diagnostic

- X-ray temperatures trace pre-shock wind velocities
- periodic X-ray variability traces the orbit
- X-ray line variations traces the flow & orientation of shocked gas



500 day merged HLGS 100 keV image, direct Chandra-like color X-ray image (0.3-0.5 keV) from 0.524-0.528, 0.532-0.536, 0.540-0.544, and 0.548-0.552 days (Smith and J. Morse)

X-rays are generated in the shock where the massive, slow wind from Eta Car smashes into and overcomes the thin fast wind from the companion.

$$\frac{p_{\text{wind},i}}{p_{\text{wind},c}} = \frac{M_i V_{\infty,i}}{M_c V_{\infty,c}}$$

force balance determines which wind dominates

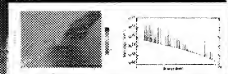
$$L_x \propto n^2 v \propto \frac{M^2}{D}$$

intrinsic X-ray luminosity is proportional to the square of the density

$$L_{x,\text{obs}} \propto L_x e^{-\alpha N_H}$$

observed flux is the intrinsic flux times the absorption

IXTE lightcurve of Eta Car, with times of Chandra observations

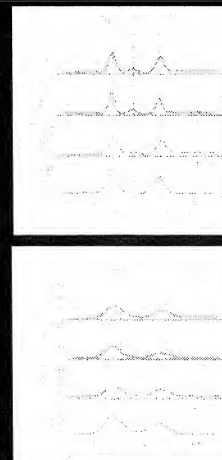


numerical hydro model of Eta Car CW and intrinsic X-ray spectrum



JD = 2,400,000

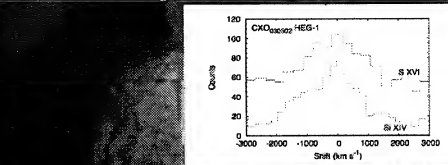
Line Profile Variations from the HETG:



Helium-like lines

Left: the variation of the Si XIII triplet from phase=0.528 (near apastron) to phase=0.992 (just before X-ray minimum, near periastron). The R ratios are consistent with the low density/low photoexcitation limit, although the lines broaden and become more blue-shifted near periastron.

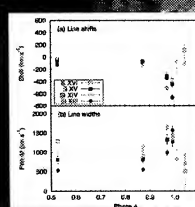
Above: the Fe XXV triplet blend shows increasingly strong "red wing" near



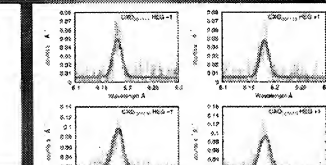
Hydrogen-like lines

Left: the variation of the Si XIV vs. phase. The lines broaden and shift in centroid velocity. The lines show the profiles from the model described below.

Above: Comparison of the Si XIV and S XVI lines at phase=0.97, near X-ray maximum



Variations in shifts and widths; lines in gray are contaminated by the CCE (Hamaguchi et al., 2007, ApJ, in press)



Profile colors: Corcoran et al. (2001, ApJ 547, 1034); Smith et al. (2004, ApJ, 610, L105); Henley et al. (2007, ApJ, submitted)

A Model of the Colliding Wind Flow

We modeled the colliding wind flow as a series of cylindrically-symmetric rings using:

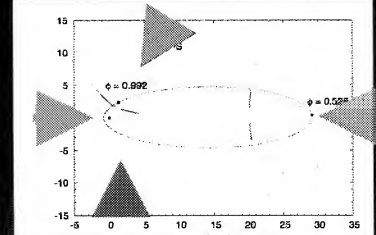
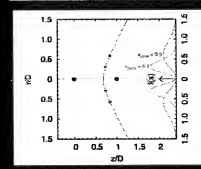
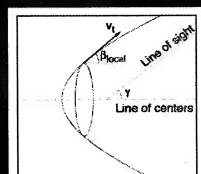
- the Canto, Raga and Wilkin (1996) wind-wind interaction geometry, with a scale factor to describe the Canto et al. flow velocity in each ring
- emissivity given by

$$e(v) \propto v_f \sin^2 \beta_{\text{local}} \sin^2 \gamma - (v + v_f \cos \beta_{\text{local}} \cos \gamma)^2 - 1/2$$

- line luminosity vs. position x along the shock based on hydrodynamical models

$$l(x) \propto \frac{1}{\sqrt{\pi} x_{\text{peak}}^2} L_{\text{line}} x^2 e^{(-x/x_{\text{peak}})^2}$$

where x_{peak} is the peak of the emission, and L_{line} the total line luminosity. The line profiles for 3 longitudes of periastron are



Lines of sight for 4 longitudes of periastron: Corcoran et al. (2001, ApJ 547, 1034); Smith et al. (2004, ApJ, 610, L105); Abraham et al. (2005, MN, 364, 922); Henley et al. (2007, ApJ, submitted)